

## **CREEP DEFORMATION IN TERMS OF SYNTHETIC THEORY**

**A. RUSINKO**

Óbuda University  
Népszínház St. 8, 1081, Budapest  
Hungary  
e-mail: rusinko.endre@bgtk.uni-obuda.hu

### **Abstract**

The paper concerns with the generalization of synthetic theory to the modelling of both plastic and creep deformations, as well as the interrelation between them. Together with the modelling of conventional creep, non-classical problems such as creep delay and creep with different plastic pre-strains are considered, which grow out of the competency of the classical theories of plasticity and creep. Results obtained in terms of the generalized synthetic theory show satisfactory agreement with experiments.

### **1. Introduction**

The work presented herein regards the generalization of the synthetic theory of plastic deformation presented in the work of Rusinko and Rusinko [21] to the modelling of not only plastic, but also creep (both primary and steady-state) deformation, as well as the plastic-creep deformation interrelation. The key points of the generalized synthetic theory are:

---

Keywords and phrases: plastic deformation, primary creep, steady-state creep, plastic-creep strain interrelation.

Received January 28, 2010

I. It is of both mathematical and physical nature. As a mathematical (formal) model, the synthetic theory is in full agreement with basic laws and principles of plasticity such as Drucker's postulate, the law of the deviator proportionality, isotropy postulate, etc. (Rusinko and Rusinko [21]).

On the other hand, the synthetic theory is a physical one, which includes the characteristics of the microstructure of metal (the nucleation and evolution of crystal lattice defects) and their interplay with microscopic and macroscopic plastic flow. This is motivated by that classical plasticity ignores completely the microstructure and its evolution in the course of plastic flow, yet the evolution of microstructure is the reason for work hardening and many other plasticity and creep phenomena. Being of two-level nature, the synthetic theory is akin to the crystal plasticity theories (Asaro [4], Hutchinson [10], Nemat-Nasser and Okinaka [14]). The key question is: which mechanisms of the act of plastic/creep deformation should be taken into account, and in what manner plastic microstrains should be connected to their carriers, the defects of crystal lattice? For the basic mechanism of irreversible strain, we take a slip of the parts of crystal grains relative to each other. To model microstrains vs. defects relation, we focus only on incontrovertible facts about in what interplay the defects of crystal lattice and plastic/creep straining are, while those of secondary importance are omitted from consideration. This makes possible to introduce relatively simple relations on the micro-level of material which, at the same time, adequately reflect the real behavior of material in unrecoverable (permanent) deforming. An excessive concretization of the mechanisms, which accompany/induce irreversible deformation inevitably leads to extremely cumbersome expressions, in which the role of the dominating processes can be unjustifiably veiled.

Summarizing, the synthetic theory is aimed to strike a compromise between a physical adequacy, and simplicity in calculations to be more readily applied to engineering design (Rusinko [22]).

II. Independently on the type of deformation (creep or plastic) to be modelled, a single notion, irreversible (permanent) deformation, is

introduced, i.e., the deformation is not splitted into plastic (instantaneous) and creep (viscous) parts (Rusinko [19, 20]). The manifestation of plastic or creep component and their interrelations depend on concrete loading- and temperature-regimes. The correctness to use the notion of irreversible deformation follows from the similarity of the mechanism of time-dependent and plastic deformation. Indeed, this mechanism is a slip of the parts of crystal grains relative to each other. These slips are induced mainly by the motions of dislocations which, in turn, are induced/accompanied by other micro-structural imperfections (defects) of crystalline lattice (vacancies, interstitial atoms, etc.). Undoubtedly, the driving forces and configurations of defects are different under different conditions. Nevertheless, despite of the variety of processes occurring in a body subjected to different loading regimes, numerous experiments systematically record the arising of dislocation gliding for any type of inelastic straining. Other facts justifying the similarity of the nature of plastic and time-dependent deformation are (i) a hydrostatic stress does not affect creep deformation; (ii) the axes of principal stress and creep strain rate coincide; (iii) no volume change occurs during creep (Bethen [5]). These observations are the same as those for plastic deformation (Chen and Han [9], Chakrabarty [8]).

III. Following the tendency of unified approaches to the determination of irreversible deformation (see, e.g., Chaboche et al. [6, 7]), the system of constitutive equations that governs the whole spectrum of inelastic deformation has been worked out. In terms of generalized synthetic theory, the universality of this system is based on following:

(i) a single equation provides the relation between (a) micro-irreversible-deformation, (b) defects of crystalline structure inducing this deformation, and (c) time. Further, the procedure of the transition from micro-to macro-level is also uniformed: irreversible macro-strains are calculated as the sum of the corresponding irreversible micro-strains.

(ii) a hardening rule is set in such a way that, the transformation of loading surface obeys an unique rule; in addition, the kinetics of the loading surface transformation is not set a priori, but is fully determined by loading trajectory.

The objectives of this paper are to demonstrate how, by utilizing the uniformed method, the generalized synthetic theory is capable of embracing both plastic and creep deformation. In addition, the problem of the interrelation between plastic and creep deformation, i.e., creep deformation with different plastic pre-strains, is considered. This problem, which grows out of the competency of classical theories, remains a challenging open one; experiments performed by Ohashi et al. [15] refute the erroneous conjecture that plastic and creep deformations do not affect each other, and thus must be described by separate models. The results of Ohashi et al. [15] contradict the hypothesis of creep potential (Bethen [5], Rabotnov [17]) that defines the creep strain as a single-valued function of the acting stress and temperature independently on loading prehistory. Another phenomenon, creep delay, which under certain conditions accompanies creep, is modelled.

## 2. Fundamentals of the Synthetic Theory of Plastic Deformation

The synthetic theory, concerned only with small plastic strains, falls within the category of work-hardening theories of plasticity. Below, the basic principles of the synthetic theory (Rusinko and Rusinko [21]) are briefly reviewed.

**(A)** The establishment of strain-stress relationships takes place in the Ilyushin stress deviatoric space,  $\mathbf{S}^5$ , (Ilyushin [11]). A load is presented by stress-deviator vector,  $\bar{\mathbf{S}}$ , whose components are

$$\begin{aligned} S_1 &= \sqrt{3/2}S_{xx}, & S_2 &= S_{xx}/\sqrt{2} + \sqrt{2}S_{yy}, \\ S_3 &= \sqrt{2}S_{xz}, & S_4 &= \sqrt{2}S_{xy}, & S_5 &= \sqrt{2}S_{yz}, \end{aligned} \quad (2.1)$$

where  $S_{ij}$  ( $i, j = x, y, z$ ) are the stress-deviator tensor components;  $|\bar{\mathbf{S}}| = 3\sqrt{2}J_2$ , where  $J_2$  is the second invariant of stress deviator tensor (Chen and Han [9]). Further throughout, we will consider the cases when  $\bar{\mathbf{S}} \in \mathbf{S}^3$  ( $S_4 = S_5 = 0$ ).

**(B) Yield criterion and yield surface.** One of the key points consists in the construction of planes tangential to yield surface in  $\mathbf{S}^5$ , instead of the yield surface itself. The inner-envelope of tangent planes constitutes the yield surface. By making use of this method, a new yield criterion is introduced, which coincides with neither the Tresca nor von-Mises yield criterion in  $\mathbf{S}^5$ . At the same time, the new criterion is reduced to the von-Mises yield criterion in  $\mathbf{S}^3$ , meaning that the trace of the five-dimensional yield surface takes the form of sphere in  $\mathbf{S}^3$ :

$$S_1^2 + S_2^2 + S_3^2 = S_S^2, \quad S_S = \sqrt{2}\tau_S, \quad (2.2)$$

where  $\tau_S$  is the yield limit of material in pure shear.

**(C) Loading surface.** During loading, the stress deviator vector shifts on its endpoint planes tangential to the yield surface in  $\mathbf{S}^5$ . The movements of the planes located on the end-point of stress deviator vector are translational, i.e., without a change of their orientations. Those planes, which are not on the endpoint of stress deviator vector remain unmovable. Despite the fact  $\bar{\mathbf{S}} \in \mathbf{S}^3$ , the displacements of planes tangential to the **five-dimensional yield surface** must be considered. On the other hand, the positions of planes tangential to the five-dimensional yield surface can be set by their traces in  $\mathbf{S}^3$ . As a result (Rusinko and Rusinko [21]), any plane locating beyond the sphere (2.2) is the trace of plane tangential to the five-dimensional yield surface.

The loading surface constructed as an inner-envelope of tangent planes takes the shape fully determined by the current positions of planes. Therefore, the behavior of loading surface is not prescribed a priori, but is fully determined by the hodograph of stress deviator vector.

Figure 1(a) illustrates the yield surface (circle) (2.2) in  $S_1$ - $S_2$  coordinate-plane at the virgin state of material, while Figure 1(b) shows the loading surface due to the action of stress deviator vector. The planes (lines) tangential both to the five-dimensional yield surface and its traces are shown in black. The lines filling up  $S_1$ - $S_2$  plane beyond the circle (the

traces of planes tangential to the five-dimensional yield surface) are shown in grey. The tangent lines incurring displacements on the end-point of vector  $\vec{\bar{S}}$ , and the loading surface as their inner-envelope are shown in red in Figure 1(b). It is easy to see (Figure 1(b)) that a corner point arises on the loading surface at the end-point of  $\vec{\bar{S}}$  (loading point). This fact is of great importance for the description of the peculiarities of plastic straining at non-smooth (orthogonal) loading trajectories (Rusinko and Rusinko [21]), where any theory with regular loading surface has proved to be unsuitable.

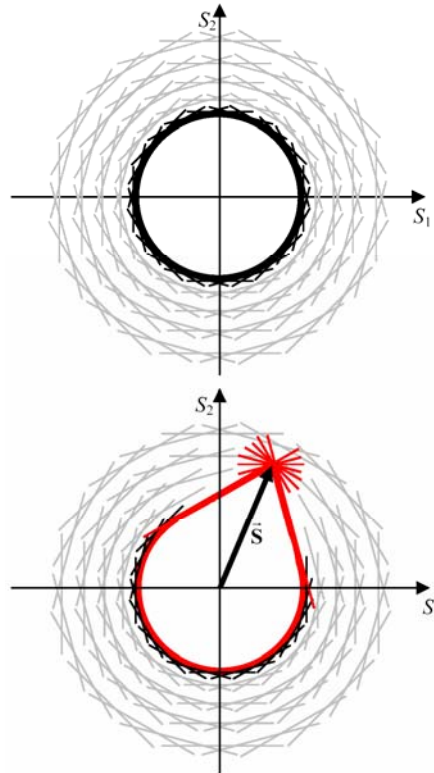


**Figure 1.** Yield and loading surface in terms of synthetic theory.

The condition that a tangent plane is located on the end-point of  $\vec{\mathbf{S}}$ , can be expressed as

$$H_N = \vec{\mathbf{S}} \cdot \vec{\mathbf{N}}, \quad (2.3)$$

where  $H_N$  is the distance between the origin of coordinates and the tangent plane in  $\mathbf{S}^5$ ;  $\vec{\mathbf{N}}$  is the unit vector normal to the tangent plane, which defines the orientation of the plane. If the plane is not reached by  $\vec{\mathbf{S}}$ ,  $H_N > \vec{\mathbf{S}} \cdot \vec{\mathbf{N}}$ . The distance to plane in  $\mathbf{S}^5$  can be expressed through that to its trace in  $\mathbf{S}^3$ ,  $h_m$ , as (Rusinko and Rusinko [21])

$$H_N = h_m \cos \lambda, \quad (2.4)$$

where index  $m$  indicates the unit vector,  $\vec{\mathbf{m}}$ , normal to the tangent plane in  $\mathbf{S}^3$ :

$$\vec{\mathbf{m}}(\cos \alpha \cos \beta, \sin \alpha \cos \beta, \sin \beta), \quad (2.5)$$

and  $\lambda$  is the angle between the vectors  $\vec{\mathbf{m}}$  and  $\vec{\mathbf{N}}$ . Components  $N_k$  and  $m_k$  are related to each other as

$$N_k = m_k \cos \lambda, \quad (k = 1, 2, 3) : N_1 = \cos \alpha \cos \beta \cos \lambda, \quad N_2 = \sin \alpha \cos \beta \cos \lambda, \\ N_3 = \sin \beta \cos \lambda. \quad (2.6)$$

Therefore, Equations (2.3) and (2.6) give that

$$H_N = \vec{\mathbf{S}} \cdot \vec{\mathbf{m}} \cos \lambda = (S_1 m_1 + S_2 m_2 + S_3 m_3) \cos \lambda, \quad \vec{\mathbf{S}} \in \mathbf{S}^3. \quad (2.7)$$

As follows from Equations (2.4) and (2.6), if  $\lambda = 0$ , then  $H_N = h_m$  and  $N_k = m_k (k = 1, 2, 3)$ . This holds true for the planes, which are tangential both to the five-dimensional yield surface and sphere (2.2). It is these planes with  $\lambda = 0$ , that govern the transformation of loading surface in  $\mathbf{S}^3$ .

**(D) Plastic strain vector components.** Similarly to the *Batdorf-Budiansky slip concept*, the synthetic theory is of two-level nature.

Each tangent plane represents an appropriate slip system (microlevel) at a point in body, and the plane motion symbolizes an elementary process of plastic deformation within this slip system. To define an average continuous measure of plastic slip within one slip system, we introduce a scalar magnitude,  $\varphi_N$ ,

$$r\varphi_N = H_N - \sqrt{2}\tau_S = \bar{\mathbf{S}} \cdot \bar{\mathbf{N}} - \sqrt{2}\tau_S, \quad (2.8)$$

which is called the *plastic strain intensity*. Equation (2.8) holds true for the plane displaced by stress deviator vector, i.e., if  $H_N = \bar{\mathbf{S}} \cdot \bar{\mathbf{N}}$ . If  $H_N > \bar{\mathbf{S}} \cdot \bar{\mathbf{N}}$ ,  $\varphi_N$  is set to be zero. An incremental plastic strain-vector,  $d\bar{\mathbf{e}}^S$ , (micro plastic deformation on lower (micro)-level) is assumed to be in the direction of the outer normal to the plane and determined as

$$d\bar{\mathbf{e}}^S = \varphi_N \bar{\mathbf{N}} dV. \quad (2.9)$$

In Equation (2.9),  $dV$  is an elementary volume constituted by the elementary set of planes in  $\mathbf{S}^3$  that covered an elementary distance due to infinitesimal increase in stress vector (Andrusik and Rusinko [1]):

$$dV = \cos \beta d\alpha d\beta d\lambda. \quad (2.10)$$

The total (macro) strain-vector at a point in a body,  $\bar{\mathbf{e}}^S$ , is determined as the sum (three-folded integral) of the micro strains ‘produced’ by movable planes:

$$\bar{\mathbf{e}}^S = \int_V \varphi_N \bar{\mathbf{N}} dV \quad \text{or} \quad \dot{\bar{\mathbf{e}}}^S = \int_V \dot{\varphi}_N \bar{\mathbf{N}} dV. \quad (2.11)$$

The strain vector components related to the strain-deviator tensor components  $e_{ij}$  as (Ilyushin [11])

$$\begin{aligned} e_1 &= \sqrt{3/2}e_{xx}, & e_2 &= e_{xx} / \sqrt{2} + \sqrt{2}e_{yy}, \\ e_3 &= \sqrt{2}e_{xz}, & e_4 &= \sqrt{2}e_{xy}, & e_5 &= \sqrt{2}e_{yz}. \end{aligned} \quad (2.12)$$



By using Equations (2.6) and (2.10), Equation (2.11) becomes

$$e_k^S = \int_{\alpha} \int_{\beta} \int_{\lambda} \varphi_N m_k \cos \lambda \cos \beta d\alpha d\beta d\lambda, \quad \text{or}$$

$$\dot{e}_k^S = \int_{\alpha} \int_{\beta} \int_{\lambda} \dot{\varphi}_N m_k \cos \lambda \cos \beta d\alpha d\beta d\lambda, \quad k = 1, 2, 3. \quad (2.13)$$

The integration in Equation (2.13) must be taken over planes shifted by stress deviator vector.

### 3. The Generalization of Synthetic Theory

To extend the physical base and boundaries of applicability of synthetic theory, the following is proposed.

(I) To reflect the well-known fact that the defects of metal-crystal-structure are the **carriers** of irreversible (plastic or creep) deformation, a defect intensity,  $\Psi_N$ , is introduced.  $\Psi_N$  represents an average continuous measure of defects (dislocations, vacancies, etc.) generated by irreversible deformation within one slip system.

(II) To model a primary creep and the influence of loading rate upon irreversible straining, a new function of time and loading rate, so called integral of non-homogeneity, ( $I_N$ ), is introduced. By utilizing the physical grounds of irreversible deforming, the form of  $I_N$  will be strictly derived below.

(III) Instead of Equation (2.8), the defect intensity is related to plane distances and the integral of non-homogeneity as:

$$\Psi_N = H_N - I_N - \sqrt{2}\tau_P = \bar{\mathbf{S}} \cdot \bar{\mathbf{N}} - I_N - \sqrt{2}\tau_P, \quad (3.1)$$

furthermore, if  $H_N > \bar{\mathbf{S}} \cdot \bar{\mathbf{N}}$ , we set  $\Psi_N = 0$ . The establishment of relation between  $\Psi_N$  and  $H_N$  is fully logical due to the distance  $H_N$  characterizes the degree of work-hardening. Indeed, the greater plane

distance  $H_N$ , the greater stress deviator vector is needed to reach the plane and induce irreversible strain. In Equation (3.1),  $\tau_P$  is the creep limit of material in pure shear; in terms of the generalized synthetic theory, the yield limit and creep limit are related to each other via  $I_N$  (see Section 4).

Without specifying the types of defects induced by irreversible strain, Equation (3.1) expresses an absolutely correct assertion (confirmed by an enormous number of experiments): the crystal structure defects are related to the work-hardening of material ( $H_N$ ) and rate-effects ( $I_N$ ).

(IV) To establish a relationship between irreversible deformation, defects and time ( $t$ ), the following equation is proposed

$$d\Psi_N = r d\varphi_N - K_{\Psi_N} dt, \quad (3.2)$$

where  $r$  is the model constant and  $K$  is a function of homological temperature, and the module of stress deviator tensor, whose form will be published elsewhere (an important point is that  $K = const$ , under the condition of creep straining). The units of quantities in Equation (3.2) are  $[\Psi_N] = \text{Pa}$ ,  $[\varphi_N] = 1$ ,  $[r] = \text{Pa}$ , and  $[K] = \text{sec}^{-1}$ .

In what follows, the establishment of the form of the integral of non-homogeneity, and the detailed analysis of the proposed generalizations are considered.

### 3.1. The integral of non-homogeneity

#### 3.1.1. Local micro-stresses and the physics of primary creep.

It is well known that a plastic deformation is accompanied by the formation of dislocation pile-ups, tangles of dislocations, unmovable jogs, grains boundaries, etc. (the nucleation of dislocations is observed at elastic deformation as well). These defect-formations, being of strongly local character, cause an uneven stress/strain distribution through the microstructure of metal that, in turn, leads to considerable distortions of crystal lattice, where the strain energy is mainly stored.

The considerable non-homogeneity and concentration of micro-strains/stresses of the second and third kind was observed in the experiments carried out by Kuksa et al. [12], which were performed on the specimens of pure copper, iron, and titanium in uniaxial tension producing stresses in elastic and plastic ranges. The experiments show that both stresses and strains are distributed in a strongly inhomogeneous way through the crystal grains; local peak stresses can take considerable values. In addition, if a strain is larger than the average, then the stress inducing this strain is smaller than average stress and vice versa. At the same time, the total over- and under-loading is equal to zero.

The inhomogeneous stress distribution makes a metal more unstable than in annealed state. Once favorable conditions arise (for example, if to stop the increase in stress as in creep tests), the crystal lattice distortions start to relax. In other word, the energy stored during plastic loading starts to release under a constant stress giving rise to the primary creep. It is the difference between the local and average stresses is the driving force for the relaxation, which occurs mainly due to spontaneous slips in grains induced by the movements of dislocation. Indeed, under thermal fluctuations, locked and tangled dislocations, and the obstructions in their way themselves become progressively movable thereby causing the development of primary creep deformation.

The local stresses arising around the lattice distortions, we will call local peak micro-stresses. These stresses display the following properties (Asaro and Rice [2], Peirce et al. [16]): (1) they, being directly correlated with dislocation density, make a material stronger; (2) the larger loading rate, the larger local stresses; and (3) they are unstable, as soon as favorable conditions arise, they decrease with time. It must be noted that, the local micro-stress relaxation is also observed during slow loading.

Therefore, on the one hand, the local micro-stresses cause the “rate-hardening” of material during active loading but, on the other hand, they can relax resulting in the softening of the material. The time-dependent macrodeformation of material is the result of the concurring processes of the hardening and softening.

### 3.1.2. The integral of non-homogeneity as the mathematical measure of local peak stresses

The integral of non-homogeneity is obtained on the base of the statistical analyze of the influence of micro-stress distribution upon the elastic strain energy of material. For this purpose, consider an elementary volume of body (treated as point) consisting of a large number of microparticles (grains). Let  $\bar{\sigma}_{kq}^0$  denote the average stress deviator tensor components (macro-stress) acting at the given point. The micro-stress non-homogeneity can be expressed through the stress deviator tensor components acting in each microparticle,  $\bar{\sigma}_{kq}$ , as

$$\bar{\sigma}_{kq} = \bar{\sigma}_{kq}^0 + \bar{\sigma}_{kq}' , \quad (3.3)$$

where  $\bar{\sigma}_{kq}'$  are random quantities expressing an over/under-loading in each particle. We set the relation between  $d\bar{\sigma}_{kq}'$  and  $d\bar{\sigma}_{kq}^0$  as

$$d\bar{\sigma}_{kq}' = C_{ijkl} d\bar{\sigma}_{ij}^0 , \quad (3.4)$$

where  $C_{ijkl}$  are random numbers, that vary from particle to particle, which are assumed to be independent from  $\bar{\sigma}_{ij}^0$ . Let us suppose that all random numbers  $C_{ijkl}$  have an identical distribution function,  $F$ , and are independent of each other. Since  $d\bar{\sigma}_{ij}^0$  are macroscopic (average) stress components, the mathematical expectation of parameters  $C_{ijkl}$  is

$$\int_{-\infty}^{\infty} C_{ijkl} F(C_{ijkl}) dC_{ijkl} = 0 \quad \Sigma \quad (3.5)$$

meaning that the total over-and under-loading with respect to the average stress is equal to zero. In addition,

$$\int_{-\infty}^{\infty} F(C_{ijkl}) dC_{ijkl} = 1 \quad \Sigma . \quad (3.6)$$

As it was pointed out earlier, the local stresses are unstable and can relax. Let us present the equation to govern their time-dependent behavior as

$$d\bar{\sigma}_{ij}' = C_{ijpq} d\bar{\sigma}_{pq}^0 - p\bar{\sigma}_{ij}' dt. \quad (3.7)$$

The first term in the right-hand side in the above formula characterizes the increment in  $\bar{\sigma}_{ij}'$  given by Equation (3.4), while the second one,  $-p\bar{\sigma}_{ij}' dt$ , gives the time-dependent decrease of micro-stresses, which is taken to be proportional to  $\bar{\sigma}_{ij}'$ . The solution of the obtained differential equation (3.7) for  $\bar{\sigma}_{ij}'$  is

$$\bar{\sigma}_{ij}' = C_{ijkq} I_{kq}(t), \quad I_{kq}(t) = \int_0^t \frac{d\bar{\sigma}_{kq}^0}{ds} \exp(-p(t-s)) ds, \quad (3.8)$$

and Equation (3.3) becomes

$$\bar{\sigma}_{ij} = \bar{\sigma}_{ij}^0 + C_{ijkq} I_{kq}(t). \quad (3.9)$$

Substituting stresses  $\bar{\sigma}_{ij}$  from Equation (3.9) into the formula for elastic strain energy,

$$U = \frac{1}{12G} \left[ (\bar{\sigma}_{xz} - \bar{\sigma}_{yy})^2 + (\bar{\sigma}_{yy} - \bar{\sigma}_{zz})^2 + (\bar{\sigma}_{zz} - \bar{\sigma}_{xx})^2 + 6(\tau_{xy}^2 + \tau_{yz}^2 + \tau_{zx}^2) \right], \quad (3.10)$$

leads to the following relation

$$\begin{aligned} U = \frac{1}{12G} & \left\{ (\bar{\sigma}_{xx}^0 + C_{xxkq} I_{kq} - \bar{\sigma}_{yy}^0 - C_{yykq} I_{kq})^2 + (\bar{\sigma}_{yy}^0 + C_{yykq} I_{kq} - \bar{\sigma}_{zz}^0 - C_{zzkq} I_{kq})^2 \right. \\ & + (\bar{\sigma}_{zz}^0 + C_{zzkq} I_{kq} - \bar{\sigma}_{xx}^0 - C_{xxkq} I_{kq})^2 + 6 \left[ (\tau_{xy}^0 + C_{xykq} I_{kq})^2 \right. \\ & \left. \left. + (\tau_{yz}^0 + C_{yzkq} I_{kq})^2 + (\tau_{xz}^0 + C_{xzkq} I_{kq})^2 \right] \right\}. \quad (3.11) \end{aligned}$$

The mean value of  $U$  is determined by the following relation

$$\langle U \rangle = \int_{-\infty}^{\infty} \dots \int_{-\infty}^{\infty} U F(C_{xxxx}) \dots F(C_{xzxz}) dC_{xxxx} \dots dC_{xzxz}, \quad (3.12)$$

which can be decomposed in two parts

$$\langle U \rangle = J_1 + J_2, \quad (3.13)$$

$$J_1 = \int_{-\infty}^{\infty} \dots \int_{-\infty}^{\infty} U_0 F(C_{xxxx}) \dots F(C_{xzxz}) dC_{xxxx} \dots dC_{xzxz} = U_0, \quad (3.14)$$

where  $U_0$  is the strain energy for the case of homogeneous stress distribution determined by Equation (3.10) at  $\bar{\sigma}_{ij} = \bar{\sigma}_{ij}^0$ . At arriving at the result (3.14), Equation (3.6) has been taken into account. Further, in order to evaluate integral  $J_2$ ,

$$\begin{aligned} J_2 &= \frac{1}{12G} \int_{-\infty}^{\infty} \dots \int_{-\infty}^{\infty} (C_{xxxx}^2 I_{xx}^2 + 2C_{xxxx} I_{xx} \bar{\sigma}_{xx}^0 + \dots) F(C_{xxxx}) \dots F(C_{xzxz}) \\ &\quad \times dC_{xxxx} \dots dC_{xzxz} \\ &= \frac{1}{12G} I_{xx}^2 \int_{-\infty}^{\infty} C_{xxxx}^2 F(C_{xxxx}) dC_{xxxx} \cdot \underbrace{\int_{-\infty}^{\infty} \dots \int_{-\infty}^{\infty} F(C_{xxxy}) \dots F(C_{xzxz}) dC_{xxxy} \dots dC_{xzxz}}_{35} \\ &\quad + \frac{1}{6G} I_{xx} \bar{\sigma}_{xx}^0 \int_{-\infty}^{\infty} C_{xxxx} F(C_{xxxx}) dC_{xxxx} \cdot \underbrace{\int_{-\infty}^{\infty} \dots \int_{-\infty}^{\infty} F(C_{xxxy}) \dots F(C_{xzxz})}_{35} \\ &\quad \times dC_{xxxy} \dots dC_{xzxz} + \dots, \end{aligned} \quad (3.15)$$

it is enough to investigate its first two terms. Equation (3.5) implies that all the integrals in Equation (3.15) containing  $C_{ijkl}$  are equal to zero. The integrals containing  $C_{ijkl}^2$  give the variance of random numbers  $C_{ijkl}$ ,  $B_1$ :

$$\int_{-\infty}^{\infty} C_{ijkl}^2 F(C_{ijkl}) dC_{ijkl} = B_1 \Sigma. \quad (3.16)$$

As a result,  $J_2 = \frac{2B_1}{G} (I_{xx}^2 + I_{yy}^2 + I_{zz}^2 + 2I_{xy}^2 + 2I_{yz}^2 + 2I_{zx}^2)$ . Finally, Equation (3.13) becomes

$$\langle U \rangle = U_0 + \frac{2B_1}{G} (I_{xx}^2 + I_{yy}^2 + I_{zz}^2 + 2I_{xy}^2 + 2I_{yz}^2 + 2I_{zx}^2). \quad (3.17)$$

By subtracting from the right-hand side in Equation (3.17), the expression  $2B_1 / 3G (I_{xx} + I_{yy} + I_{zz})^2$ , which is equal to zero due to  $\bar{\sigma}_x^0 + \bar{\sigma}_y^0 + \bar{\sigma}_z^0 = 0$ , we obtain

$$\langle U \rangle = U_0 + \frac{2B_1}{3G} \left[ (I_{xx} - I_{yy})^2 + (I_{yy} - I_{zz})^2 + (I_{zz} - I_{xx})^2 + 6(I_{xy}^2 + I_{yz}^2 + I_{zx}^2) \right]. \quad (3.18)$$

Substituting  $I_{ij}$  from Equation (3.8) into Equation (3.18), and converting the variables  $\sigma_{ij}$  to the stress vector components  $S_n$  by Equation (2.1), the expression for the mathematical expectation of the elastic strain energy is obtained as

$$\langle U \rangle = U_0 + \frac{2B_1}{3G} \sum_{n=1}^5 \left[ \int_0^t \frac{dS_n}{ds} \exp(-p(t-s)) ds \right]^2. \quad (3.19)$$

The value of  $\langle U \rangle$  is seen to consist of two parts, the term  $U_0$  corresponds to homogeneous stress distribution, and the second term characterizes the time-dependent deviation of stresses from their average value. If a body is ideally homogeneous, the distribution functions  $C_{ijkl}$  degenerate in the Dirac delta-function and, according to Equation (3.16), we obtain

$B_1 = 0$ . As seen from Equation (3.19),  $\langle U \rangle$  depends not only on the rate of stress vector components  $\dot{S}_n$  at a given instant, but on its values for the whole loading history as well. For the case  $\dot{S}_n = \text{const}$ ,

$$\langle U \rangle = U_0 + \frac{2B_1}{3G} \dot{S}_n \dot{S}_n \left[ \int_0^t \exp(-p(t-s)) ds \right]^2, \quad (3.20)$$

and since  $\dot{S}_n \dot{S}_n = \dot{S}^2$  ( $S$  denotes the length of stress vector),

$$\langle U \rangle = U_0 + \frac{2B_1}{3G} \left[ \int_0^t \frac{dS}{ds} \exp(-p(t-s)) ds \right]^2. \quad (3.21)$$

For the case, if the stress deviator vector has a single non-zero component, Equations (3.19) and (3.21) are identical at variable loading rate as well. We take the square root in the right-hand side in Equation (3.21),

$$I = B \int_0^t \frac{dS}{ds} \exp(-p(t-s)) ds, \quad B = \sqrt{\frac{2B_1}{3G}} = \text{const}, \quad (3.22)$$

to be the scalar measure of micro-non-homogeneity that regulates primary creep; we will term  $I$  as the integral (parameter) of non-homogeneity. To work with the integral of non-homogeneity on the lower (micro) level of synthetic theory, we replace  $S$  in (3.22) by the scalar product  $\vec{\mathbf{S}} \cdot \vec{\mathbf{N}}$ . This replacement reflects the fact that the driving force for a plastic flow within a slip system is not the whole macro-stress vector  $\vec{\mathbf{S}}$ , but only its projection,  $\vec{\mathbf{S}} \cdot \vec{\mathbf{N}}$  (resolved stress). Thus, finally, the characteristic of local micro-stresses have the form

$$I_N = B \int_0^t \frac{d\vec{\mathbf{S}}}{ds} \cdot \vec{\mathbf{N}} \exp(-p(t-s)) ds. \quad (3.23)$$



In contrast to Equation (3.22), the adopted integral (3.23) depends on angles  $\alpha$ ,  $\beta$ , and  $\lambda$  thereby allowing for the orientation of tangent planes in the Ilyushin space. It must be noted that  $I_N$  is assumed to be zero, if  $\vec{S} \cdot \vec{N} < 0$ .

Consider the integral of non-homogeneity at the loading regime shown in Figure 2(a) ( $\vec{v} = d\vec{S}/dt = const$ ). On the first portion of the loading, Equation (3.23) gives

$$I_N(t) = B(\vec{v} \cdot \vec{N}) \int_0^t \exp(-p(t-s)) ds = \frac{B(\vec{v} \cdot \vec{N})}{p} [1 - \exp(-pt)], \quad t \in [0, t_1]. \tag{3.24}$$

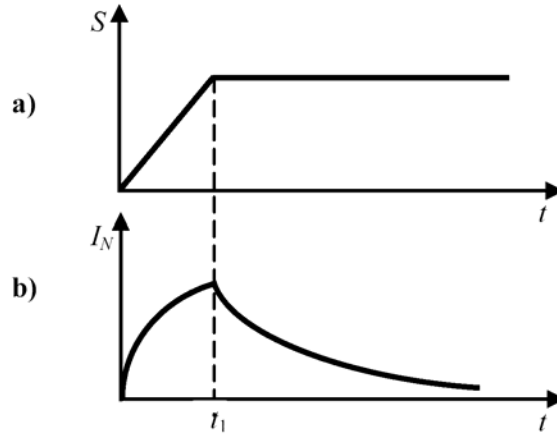


**Figure 2.**  $I_N - t$  diagram.

As seen from Equation (3.24), the integral  $I_N(t)$  grows from the very beginning of loading (Figure 2(b)). If we take the loading rate  $v = S/t$  to be infinitely large, we can approximate the function  $\exp(-pS/v)$  in Equation (3.24) by the Taylor series that results in the following relation

$$I_N = B(\vec{S} \cdot \vec{N}) \text{ as } v \rightarrow \infty. \tag{3.25}$$

For the range  $t > t_1$ , when  $\bar{\mathbf{v}} = 0$ , let us split the range of integration in Equation (3.23) into two parts, from 0 to  $t_1$  and from  $t_1$  to  $t$ . Now, Equation (3.23) becomes (the decreasing portion of  $I_N(t)$  in Figure 2(b)):

$$\begin{aligned} I_N(t) &= B(\bar{\mathbf{v}} \cdot \bar{\mathbf{N}}) \int_0^{t_1} \exp(-p(t-s)) ds \\ &= \frac{B(\bar{\mathbf{v}} \cdot \bar{\mathbf{N}})}{p} [\exp(pt_1) - 1] \exp(-pt), \quad t \geq t_1. \end{aligned} \quad (3.26)$$

If to assume the loading rate to be infinitely large, Equation (3.26) can be written as

$$I_N = B(\bar{\mathbf{S}} \cdot \bar{\mathbf{N}}) \exp(-pt). \quad (3.26a)$$

From Equations (3.24) and (3.26), the following properties of the integral of non-homogeneity can be indicated: (i) during loading, it grows proportionally to the loading rate; (ii) it decreases under constant loading. Therefore, the time-dependent behavior of the integral of non-homogeneity correlates with that of local peak micro-stresses discussed above, and regulates the rate-hardening of material.

The condition  $I_N = 0$ , symbolizes the end of transformations occurring in the crystal lattice under primary creep and the transition to the steady-state stage of creep.

### 3.2. System of constitutive equations: Loading criterion

Formulae (3.1), (3.23), (3.2), and (2.13) constitute the base of the generalized synthetic theory:

$$\psi_N = H_N - I_N - \sqrt{2}\tau_P, \quad (A)$$

$$I_N = B \int_0^t \frac{d\bar{\mathbf{S}}}{ds} \cdot \bar{\mathbf{N}} \exp(-p(t-s)) ds, \quad (B)$$

$$d\psi_N = rd\varphi_N - K\psi_N dt, \quad (C)$$

$$e_k^i = \int_{\alpha} \int_{\beta} \int_{\lambda} \varphi_N m_k \cos \lambda \cos \beta d\alpha d\beta d\lambda, \quad \text{or}$$

$$\dot{e}_k^i = \int_{\alpha} \int_{\beta} \int_{\lambda} \dot{\varphi}_N m_k \cos \lambda \cos \beta d\alpha d\beta d\lambda, \quad k = 1, 2, 3. \quad (\text{D})$$

The procedure of the calculation of irreversible strain vector components ( $e_k^i$ ) is the following,

- (i) at a given vector  $\bar{\mathbf{S}}$  and loading rate, the defect intensity  $\psi_N$  is determined by Equations (A) and (B),
- (ii) the strain intensity  $\varphi_N$  can be found by Equation (C),
- (iii) Equation (D) gives the irreversible strain (rate) vector components  $e_k^i$ .

Equation (C) is one of the most important in terms of the generalized synthetic theory. It reflects the well-known fact that the defect intensity  $d\psi_N$  grows with the increase in deformation ( $rd\varphi_N$ ) and simultaneously, decreases (relaxes) with time ( $-K\psi_N dt$ ). Owing to Equation (C), one does not need to split a deformation into its “instantaneous”(plastic) and viscous parts-both of them are developed simultaneously. The degree of this development depends on concrete loading- and temperature-regimes. That is why, further throughout, we will use a single term, irreversible deformation, by which, we mean the deformation progressing with time (independently of whether, we consider very short-termed loadings in plastic straining or the loadings lasting several hours or days as in creep tests).

The (A)-(D) system governs all types of irreversible deformation for any state of stresses and loading regimes.

Regard must be paid to the integration limits in Equation (D). When finding the boundary values of angles  $\alpha$ ,  $\beta$ , and  $\lambda$ , one must follow a single rule-only tangent planes, which are on the end-point of stress deviator tensor produce irreversible strains. Since the plane distances are

related to  $\psi_N$ , following the work of Rusinko and Rusinko [21], the limits of integration in Equation (D) are determined from the conditions  $\psi_N = 0$ ,

$$0 \leq \lambda \leq \lambda_1, \quad \cos \lambda_1(\alpha, \beta) = \frac{\sqrt{2}\tau_P}{(\bar{\mathbf{S}} \cdot \bar{\mathbf{m}}) - I_N}, \quad (3.27)$$

and condition  $\lambda_1 = 0$  gives the equation for the boundary values of angles  $\alpha$  and  $\beta$ :

$$\bar{\mathbf{S}} \cdot \bar{\mathbf{m}} - I_N = \sqrt{2}\tau_P. \quad (3.28)$$

While the limits of integration (3.27) and (3.28) can be determined relatively simply, when the loading trajectory is a straight line, it is not the case for arbitrary (curvilinear) loading paths. To express analytically, the integration limits for curvilinear loading paths is very difficult task and, consequently, computer assisted methods must be applied. Nevertheless, a general criterion for the developing of irreversible straining must be formulated. Let a current stress vector  $\bar{\mathbf{S}}$  have produced some irreversible strain, i.e., a set of tangent planes are on its end-point. For these planes, Equations (A) and (2.3) give

$$S_P + \psi_N + I_N = \bar{\mathbf{S}} \cdot \bar{\mathbf{N}}. \quad (3.29)$$

If the vector  $\bar{\mathbf{S}}$  acquires increment  $d\bar{\mathbf{S}}$ , for planes that are on the end-point of vector  $\bar{\mathbf{S}} + d\bar{\mathbf{S}}$ , we have

$$S_P + \psi_N + d\psi_N + I_N + dI_N = \bar{\mathbf{S}} \cdot \bar{\mathbf{N}} + d\bar{\mathbf{S}} \cdot \bar{\mathbf{N}}. \quad (3.30)$$

Therefore, together with Equation (3.29), we obtain that

$$d\psi_N = d\bar{\mathbf{S}} \cdot \bar{\mathbf{N}} - dI_N. \quad (3.31)$$

We propose the following criterion: the planes that produce irreversible strains due to a given vector  $\bar{\mathbf{S}}$  continue to do this due to the vector  $\bar{\mathbf{S}} + d\bar{\mathbf{S}}$ , if for these planes  $d\psi_N \geq 0$ :

$$d\vec{S} \cdot \vec{N} - dI_N \geq 0. \quad (3.32)$$

Equation (3.32), together with Equations (3.27) and (3.28), must be applied to the determination of integration limits in Equation (D).

#### 4. Creep-Yield Limit Interrelation

Consider the case of arbitrary stress state, and assume that the loading rate is infinitely small, so that the integral of non-homogeneity tends to zero. If an irreversible deformation does not occur,  $\psi_N = 0$ , Equation (A) gives that tangential planes in  $\mathbf{S}^3(\lambda = 0)$  are equidistant from the origin of coordinates:

$$h_m(\alpha, \beta) = H_N(\alpha, \beta, \lambda = 0) = \sqrt{2}\tau_P. \quad (4.1)$$

The above formula implies that the creep surface (creep locus in  $\mathbf{S}^3$  setting the condition for the onset of first plastic flow at infinitesimal loading rate), being constructed as the inner-envelope of tangential planes, takes the form of the sphere of radius  $\sqrt{2}\tau_P$ :

$$S_1^2 + S_2^2 + S_3^2 = S_P^2, \quad S_P = \sqrt{2}\tau_P, \quad (4.2)$$

Further throughout, we will use the creep surface (4.2) instead of sphere (2.2).

Let us establish relation between the yield limit and creep limit of material, between  $\tau_S$  and  $\tau_P$ . Consider the case when the length of vector  $\vec{S}$ ,  $S$ , changes in time as shown in Figure 2(a). Until stress vector reaches tangential planes (Figure 3(a)),  $\psi_N = 0$ , Equation (A) takes the form

$$H_N = I_N + S_P, \quad (4.3)$$

where  $I_N$  is given by Equation (3.24). As seen from (4.3), the plane distances grow due to the increase in  $I_N$ . This means that Equation (4.3) describes the movements of planes in the direction away from the origin of coordinate. Since these movements are not caused by the “pushing” action of stress deviator vector, they do not cause irreversible strain. The

inner envelope of planes with distances from Equation (4.3) is shown in Figure 3(a). Therefore, Figure 3(a) descriptive-geometrically shows the hardening action of the integral of non-homogeneity: the greater  $I_N$ , the greater  $H_N$  and, consequently, the greater stress is needed to induce plastic flow.

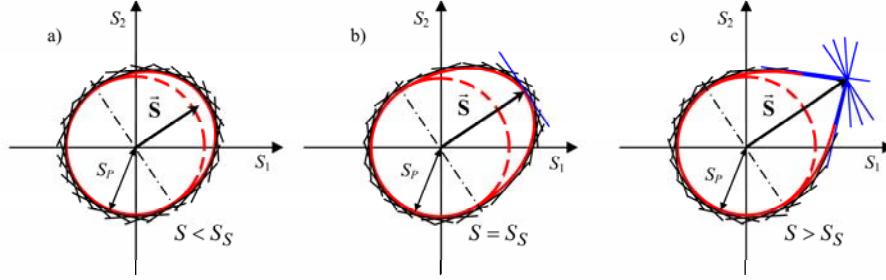


**Figure 3.** The transformation of yield (a and b) and loading surface (c) (the planes with  $\lambda = 0$  are shown only).

Let  $S_S$  denote the length of the stress deviator vector, which at time  $t_S$  ( $t_S \in [0, t_1]$  in Figure 2(a)) reaches the first plane, i.e., the plastic flow starts developing (Figure 3(b)). For this plane  $\vec{S} \cdot \vec{N} = S_S$ , and Equation (2.3) gives that  $H_N = S_S$ . The replacement of  $H_N$  by  $S_S$  in (4.3) leads to the equation for  $S_S$ :

$$S_S = \frac{Bv}{p} (1 - \exp(-pt_S)) + S_P, \quad S_S = vt_S. \quad (4.4)$$

It is easy to show that the condition that the stress vector reaches first plane can be satisfied only, if  $0 \leq B < 1$ . The plot of  $S_S$  as a function of  $v$  constructed on the base of Equation (4.4) is shown in Figure 4. As follows from Equation (4.4), curve  $S_S = S_S(S_P)$  has a horizontal asymptote, which is distant of  $S_P/(1-B)$  from the abscissa that corresponds to the case of infinite large loading rate. For  $S > S_S$ , the stress vector displaces the set of planes meaning the progress in irreversible strain (Figure 3(c)).

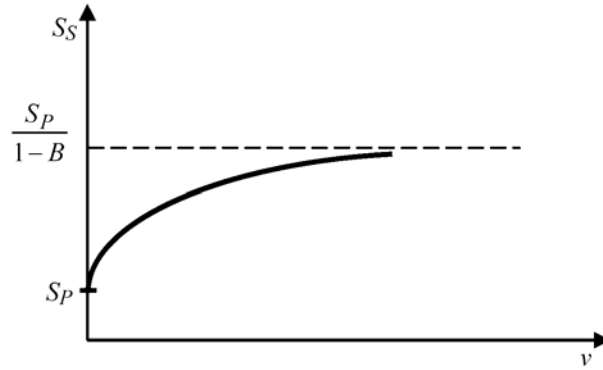


**Figure 4.** The yield limit dependence of loading rate.

### 5. Irreversible Deformation in Terms of the Generalized Synthetic Theory

Let us apply Equations (A)-(D) to the determination of irreversible deformation for the case of proportional loading, when the loading trajectory is a straight line in the Ilyushin deviator space, and function  $S(t)$  has a form as in Figure 2(a). Since the synthetic theory provides the fulfillment of the law of the deviator proportionality (Rusinko and Rusinko [21], Rusinko [18]), the formulae obtained for the case of, e.g., uniaxial tension are fully applicable (up to constants) to arbitrary, proportional loading.

For the case of uniaxial tension ( $\bar{\mathbf{S}}(S_1, 0, 0)$ ,  $S_1 = \sqrt{2/3}\sigma_x$ , see Equation (2.1)) Equation (A), together with Equations (2.5) and (2.7), gives the defect intensity as

$$\psi_N = [S_1 - I]\Omega - S_P, \quad \Omega = m_1 \cos \lambda = \cos \alpha \cos \beta \cos \lambda, \quad S_1 > S_S, \quad (5.1)$$

where, according to Equation (B),

$$I = Bv \int_0^t \exp[-p(t-s)] ds. \quad (5.2)$$

According to Equations (3.27) and (3.28), the defect intensity in Equation (5.1) is positive for

$$-\alpha_1 \leq \alpha \leq \alpha_1, \quad -\beta_1 \leq \beta \leq \beta_1, \quad 0 \leq \lambda \leq \lambda_1,$$

$$\cos\lambda_1 = \frac{S_P}{S_1(1-I)\cos\alpha\cos\beta}, \quad \cos\beta_1 = \frac{S_P}{S_1(1-I)\cos\alpha}, \quad \cos\alpha_1 = \frac{S_P}{S_1(1-I)}. \quad (5.3)$$

Beyond these ranges, we have  $\psi_N = d\psi_N = 0$  and  $\varphi_N = d\varphi_N = 0$ . The defect intensity increment is

$$d\psi_N = (dS_1 - dI)\Omega, \quad (5.4)$$

and Equation (C) gives the strain intensity as

$$rd\varphi_N = d\psi_N + K\psi_N dt = (dS_1 - dI)\Omega + K([S_1 - I]\Omega - S_P)dt. \quad (5.5)$$

To evaluate strain vector components by Equation (D), the different orders of integration in (5.5) can be applied: first, the integration over angles  $\alpha$ ,  $\beta$ , and  $\lambda$ , and then time-integration or vice versa. Both of them are presented below.

Equation (C) gives the irreversible-strain-vector-component increment,  $\Delta e_1^i$ , as

$$\Delta e_1^i = \frac{1}{2r} \int_{-\alpha_1}^{\alpha_1} \cos\alpha d\alpha \int_{-\beta_1}^{\beta_1} \sin 2\beta d\beta \int_0^{\lambda_1} \Delta\varphi_N \cos\lambda d\lambda, \quad (5.6)$$

where the  $\varphi_N$  is given by Equation (5.5) and the integration limits are from Equation (5.3). In Equation (5.6), we have introduced the symbol  $\Delta$  to distinguish the strain-intensity-increment due to time-increment from the variables over which, the integration is carried out, i.e.,  $\alpha$ ,  $\beta$ , and  $\lambda$ . By integrating over  $\alpha$ ,  $\beta$ , and  $\lambda$  in (5.6), we obtain

$$\Delta e_1^i = a_0[\Delta F(a) + KF(a)\Delta t], \quad (5.7)$$

where



$$\alpha_0 = \frac{\sqrt{2}\pi\sigma_p}{3\sqrt{3}r} = \text{const}, \quad F(a) = \frac{\arccos a}{a} - 2\sqrt{1-a^2} + a^2 \ln \frac{1+\sqrt{1-a^2}}{a},$$

$$\alpha = \frac{\sigma_P}{\sigma_x - I}, \quad F(1) = 0. \quad (5.8)$$

The function  $F$  is a decreasing function of  $a$ , Figure 5. By integrating over time in Equation (5.7), we obtain the formula for the irreversible strain component in uniaxial tension:

$$e_1^i = \alpha_0 \left[ F(a) + \int_{t_S}^t KF(a) dt \right]. \quad (5.9)$$

To evaluate the integral in Equation (5.9), one need to know the form of the function  $K(S_1(t), \Theta)$ .

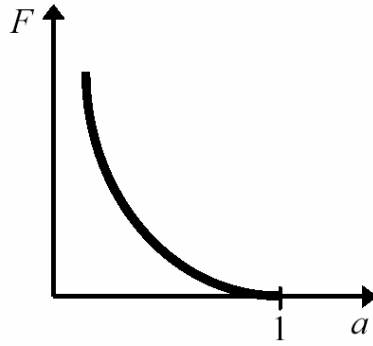


**Figure 5.**  $F(a)$  function.

Following the law of deviator proportionality (Rusinko [18]), Equation (5.9) can be rewritten for the case of arbitrary, proportional stress state as

$$e_k^i = \alpha_0 \left[ F(a) + \int_{t_S}^t KF(a) dt \right] \frac{S_k}{S}, \quad k = 1, 2, 3, \quad (5.10)$$

where, instead of (5.8),

$$a = \frac{S_P}{S - I}. \quad (5.11)$$

Equation (5.10) is of a general character: at  $t = t_1$  (Figure 2), we obtain the plastic strain vector components; at  $t > t_1$ , we get the total, plastic and creep, strain components.

### 5.1. The analysis of the system of constitutive equations: Partial cases

(1) Consider the case of steady-state creep, when  $dS = 0$  and  $I_N = 0$ . It is clear that Equation (3.31) gives  $d\psi_N = 0$ , i.e., the defect intensity (density) does not change during the steady state creep reflecting well-known fact that, steady-state creep deformation develops under the equilibrium between the processes of hardening and softening. Therefore, Equation (C) gives the constant strain intensity rate:

$$r\dot{\phi}_N = K\psi_N = \text{const}, \quad K(S, \Theta) = \text{const}. \quad (5.12)$$

Another consequence from conditions  $dS = 0$  and  $I_N = 0$  is  $a = S_P/S = \text{const}$ , and  $F(a) = \text{const}$  (see Equations (5.8) and (5.11)). According to Equation (5.10), the steady-state creep strain rate components,  $\dot{e}_k^P$ , are

$$\dot{e}_k^P = \alpha_0 K F(a) \frac{S_k}{S} = \text{const}. \quad (5.13)$$

Since the function (constant)  $K$  appears in the formula for steady-state creep rate, we can infer that it takes very small values, and the manifestation of the second term in Equation (5.10) becomes material only at long-termed loadings (as in steady-state creep).

(2) On the base of stated above, we can neglect the second term in Equation (5.10), or the term  $K\psi_N dt$  in Equation (C), when plastic or/and primary creep strains are investigated, whose durations are

considerably smaller than those of steady-state creep. This is absolutely justifiable due to the second term in Equation (5.10) is comparable with the term  $a_0 F(a)$  only at long termed loadings. Therefore, Equation (C) at  $K = 0$  is

$$rd\varphi_N = d\psi_N, \quad (5.14)$$

and Equation (5.10) gives

$$e_k^i = a_0 F(a) \frac{S_k}{S}, \quad (5.15)$$

where  $e_k^i$  is the total, plastic + primary creep, strain components. Equation (5.14) reflects another well-known fact that the increase in plastic deformation causes that in the defects of crystal lattice leading to the work-hardening of material and, consequently, the plastic deformation progress requires the increase in acting stress. As regards to primary creep, the growth of  $\psi_N$  in the course of primary creep deformation also reflects the hardening of material, which is manifested in the gradual decrease in the primary creep strain rate.

However, the simplified formula (5.14) is suitable only to the modelling of conventional plastic/creep strains, the term  $K\psi_N dt$  must be taken into account, when non-classical problems of primary creep are considered (see Subsection 5.2)

(3) Consider the case when a complete or partial unloading follows the loading, which has produced some irreversible deformation. It is clear that now  $d\varphi_N = 0$  and Equation (C) becomes

$$d\psi_N = -K\psi_N dt. \quad (5.16)$$

The solution of this differential equation is

$$\psi_N = \psi_{N_0} \exp(-Kt), \quad (5.17)$$

where  $\psi_{N_0}$  is the defect intensity accumulated during the initial irreversible, straining. Equation (5.17) describes the process of defects relaxation, whose physical adequacy is also beyond any reasonable doubt.

### 5.2. Plastic-creep deformation interrelation

On the base of Equations (A-D), by making use of the integration order in Equations (C) and (D) opposite to that considered in Subsection 5.1, let us model a conventional primary creep strain in uniaxial tension, as well as the primary creep as a function of prior plasticity.

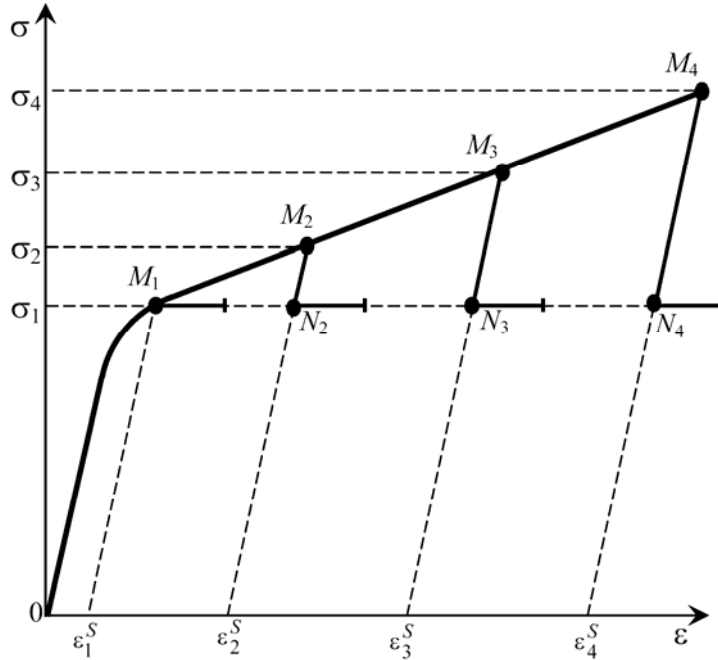


**Figure 6.** Loading regimes with different prior plasticity but equal stress in creep.

Consider the following loading regimes that precede creep straining as shown in Figure 6 (Ohashi et al. [15]). Specimen No. 1 is loaded to point  $M_1$ , the stress  $\sigma_1$  exceeds the yield strength of material, and induces plastic strain  $\varepsilon_1^S$ ; further, the stress is hold constant in time, i.e., the specimen incurs conventional creep deformation. Specimens No. 2, 3, and 4 are loaded up to stresses  $\sigma_2 < \sigma_3 < \sigma_4$  (points  $M_2$ ,  $M_3$ , and  $M_4$ ,

respectively), corresponding plastic strains are  $\varepsilon_2^S$ ,  $\varepsilon_3^S$ , and  $\varepsilon_4^S$ , then all the specimens are unloaded to the stress  $\sigma_1$  (points  $N_2$ ,  $N_3$ , and  $N_4$ ), and further, the stress is hold constant. The values of  $\sigma_j$  and  $\varepsilon_j^S$  ( $j = 1, \dots, 4$ ) are presented in Table 1 (the specimens are loaded under the temperature of  $600^\circ\text{C}$ ). Summarizing, all the four specimens incur creep deformation under the identical stress  $\sigma_1$  and temperature, but with different prior plasticity.

According to Ohashi et al. [15], the creep strains of the specimens ( $\sigma_1 = 140\text{MPa}$ ,  $t = 600^\circ\text{C}$ ) are strongly influenced by prior plasticity, namely, the greater value of plastic strain  $\varepsilon_j^S$ , the less creep strain develops (see Figure 9). Therefore, *prior plastic deformation considerably increases the resistance of material with respect to subsequent creep.*

To model, how the prior plasticity affects subsequent creep, it is enough to study the creep strains of Specimens No. 1 and No. 2.

**Specimen No. 1.** In contrast to the Subsection 5.1, we change the integration order: first, by means of time-integration in Equation (C), we obtain the strain intensity  $\varphi_N$  as a function of  $\alpha$ ,  $\beta$ , and  $\lambda$ , and then  $e_i$  components are calculated by integrating with respect to  $\alpha$ ,  $\beta$ , and  $\lambda$  in Equation (D).

Since the duration of loading/unloading (the time periods of portions  $OM_1$ ,  $OM_2$ , ... as well as  $M_2N_2$ ,  $M_3N_3$ , ...) are ignorable with respect to that of subsequent creep, the integral of non-homogeneity (5.2) takes form of Equation (3.26a) and Equations (5.1) becomes

$$\psi_N = S_1[1 - B \exp(-pt)]\Omega - S_p, \quad t \geq 0. \quad (5.18)$$

The defect intensity is non-zero within the following ranges

$$-\alpha_2 \leq \alpha \leq \alpha_2, \quad -\beta_2 \leq \beta \leq \beta_2, \quad 0 \leq \lambda \leq \lambda_2,$$

$$\cos \lambda_2 = \frac{S_P}{S_1(1 - B \exp(-pt)) \cos \alpha \cos \beta}, \quad \cos \beta_2 = \frac{S_P}{S_1(1 - B \exp(-pt)) \cos \alpha},$$

$$\cos \alpha_2 = \frac{S_P}{S_1(1 - B \exp(-pt))}, \quad t \geq 0. \quad (5.19)$$

Beyond the ranges (5.19)  $\psi_N = 0$ . The distances to planes, according to Equations (A) and (5.18), are

$$H_N = S_1 \Omega, \quad \text{for the ranges (5.19),} \quad (5.20a)$$

$$H_N = S_P + BS_1 \exp(-pt) \Omega, \quad \text{beyond the ranges (5.19).} \quad (5.20b)$$

The loading surfaces for Specimen No. 1, constructed in  $S_1$ - $S_2$  coordinate plane as the inner-envelope of tangent planes with distances governed by Equations (5.20a, b), are shown in Figure 7(a), (b) (the planes in blue are on the end-point of vector and, therefore, they “produce” the creep strain). As follows from Equation (5.20b), due to the decrease in  $BS_1 \exp(-pt) \Omega$ , the planes move toward the origin that results in the growth of the set of planes locating at the end-point of stress vector. Indeed, while the set of planes at  $t = 0$  is defined by the boundary angle  $\alpha_1$ ,  $\alpha_1 = \alpha_2(t = 0)$ , the number of planes being at the end-point of  $\bar{\mathbf{S}}$  grows:  $\alpha_2 > \alpha_1$  as  $t > 0$  (compare Figure 7(a) and 7(b)).

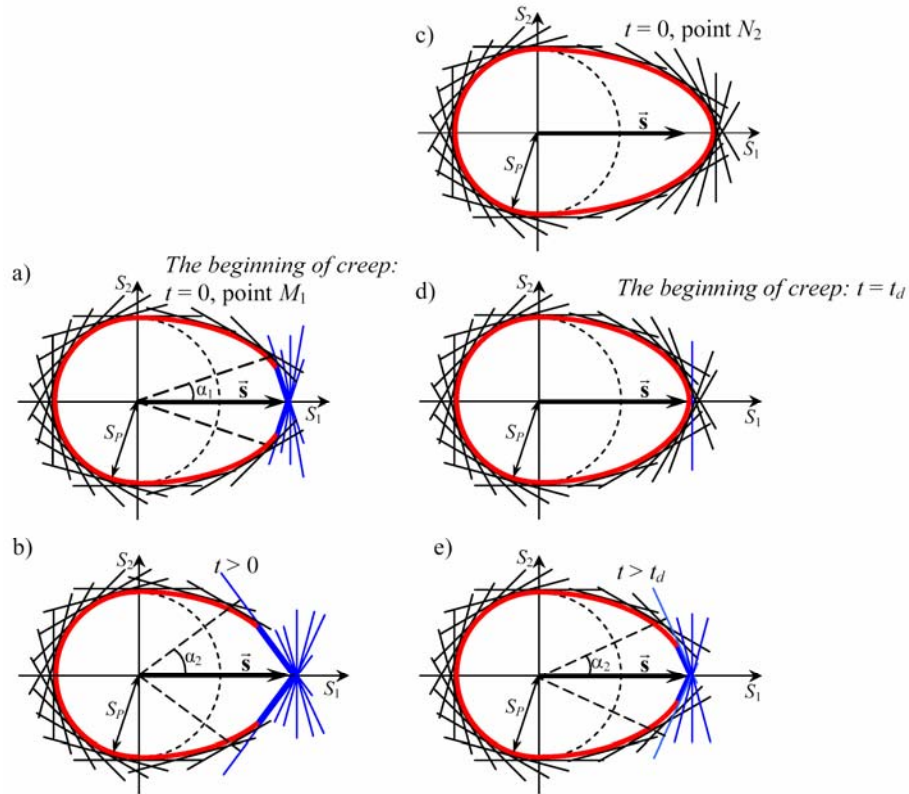


**Figure 7.** The evolution of loading surfaces for Specimens No. 1 (a, b) and No. 2 (c-e) in time (the tangent planes with  $\lambda = 0$  are shown only). The length of  $\bar{S}$  is  $S_1$ .

The decrease in the integral of non-homogeneity reflects the processes of the release of the strain energy, which is stored in material due to plastic loading, that are manifested in the increase in the number of defects capable of producing primary creep.

On the base of Equation (5.18), Equation (C) yields the following form:

$$rd\varphi_N = BS_1 p \exp(-pt)\Omega dt + K[(S_1 - BS_1 \exp(-pt))\Omega - S_P]dt. \quad (5.21)$$

To calculate the primary creep strain vector component  $e_1^P$ , one needs to integrate the  $\varphi_N$  over the range (5.19):

$$e_1^P = \int_{-\alpha_2}^{\alpha_2} \cos \alpha d\alpha \int_{-\beta_2}^{\beta_2} \cos^2 \beta d\beta \int_0^{\lambda_2} \varphi_N \cos \lambda d\lambda. \quad (5.22)$$

To do this, we split the range (5.19) into the following two domains. The first of them, domain I, is

$$-\alpha_1 \leq \alpha \leq \alpha_1, \quad -\beta_1 \leq \beta \leq \beta_1, \quad 0 \leq \lambda \leq \lambda_1, \quad t = 0, \quad (5.23)$$

where  $\alpha_1 = \alpha_2(t = 0)$ ,  $\beta_1 = \beta_2(t = 0)$ , and  $\lambda_1 = \lambda_2(t = 0)$ . Domain I corresponds to the beginning of creep (point  $M_1$ ,  $t = 0$ ). The second domain, II, is

$$\alpha_1 \leq |\alpha| \leq \alpha_2, \quad \beta_1 \leq |\beta| \leq \beta_2, \quad 0 \leq \lambda \leq \lambda_2, \quad t > 0, \quad (5.24)$$

where  $\alpha_2$ ,  $\beta_2$ , and  $\lambda_2$  are given by (5.19). It is easy to see that domain II is the extension of domain I in the course of creep strain. Taking the time integral in Equation (5.21), the creep strain intensity developed in the domain I is obtained as

$$r\varphi_{NI} = BS_1[1 - \exp(-pt)]\left(1 - \frac{K}{p}\right)\Omega + K(S_1\Omega - S_P)t, \quad t \geq 0. \quad (5.25)$$

The instant,  $t_0$ , when a plane from the region II starts producing creep strain is calculated from Equation (5.18) at  $\psi_N = 0$ :

$$S_P + BS_1\Omega \exp(-pt_0) = S_1\Omega, \quad (5.26)$$

$$t_0(\Omega) = \frac{1}{p} \ln \frac{BS_1\Omega}{S_1\Omega - S_P}. \quad (5.27)$$

Since, depending on the orientation of tangent plane from domain II, the defect intensity is non-zero for the period of time  $[t_0, t)$ , the time-integration in Equation (5.21) gives the strain intensity in domain II as

$$r\varphi_{MII} = BS_1[\exp(-pt_0) - \exp(-pt)]\left(1 - \frac{K}{p}\right)\Omega + K(S_1\Omega - S_P)(t - t_0). \quad (5.28)$$



The macro creep strain vector component is determined by the integration of  $\varphi_{NI}$  and  $\varphi_{NII}$  over the regions I and II,

$$\begin{aligned}
 e_1^P = & \int_{-\alpha_1}^{\alpha_1} \cos \alpha d\alpha \int_{-\beta_1}^{\beta_1} \cos^2 \beta d\beta \int_0^{\lambda_1} r\varphi_{NI} \cos \lambda d\lambda \\
 & + 2 \int_{\alpha_1}^{\alpha_2} \cos \alpha d\alpha \int_{-\beta_2}^{\beta_2} \cos^2 \beta d\beta \int_0^{\lambda_2} r\varphi_{NII} \cos \lambda d\lambda \\
 & + 2 \int_{-\alpha_1}^{\alpha_1} \cos \alpha d\alpha \int_{\beta_1}^{\beta_2} \cos^2 \beta d\beta \int_0^{\lambda_2} r\varphi_{NII} \cos \lambda d\lambda.
 \end{aligned}
 \tag{5.29}$$

The integrals in (5.29) can not be expressed as elementary functions; therefore, one comes to the point, where numerical computation is the only practicable way of integration.

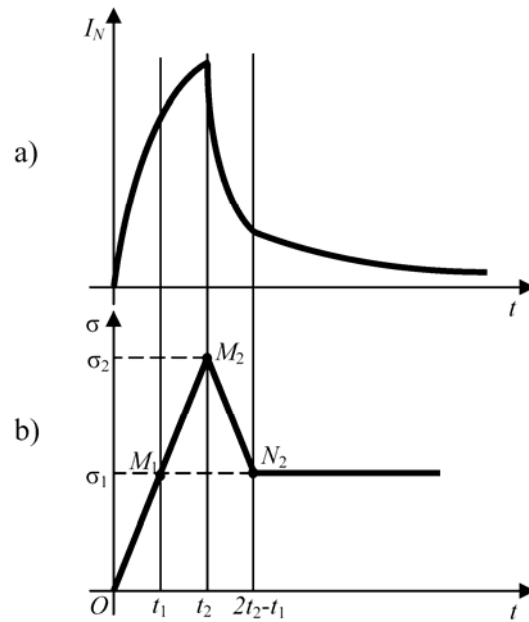


**Figure 8.** The integral of non-homogeneity at  $OM_2N_2$  loading regime.

**Specimen No. 2.** First of all, the integral of non-homogeneity for the loading pass  $OM_2N_2$  (Figure 8(b)) must be studied. Begin with, the loading/unloading rate is assumed to be of finite magnitude. Equation (B) gives

$$I_N = Bv \left[ \int_0^{t_2} \exp(-p(t-s)) ds \right] \Omega = \frac{Bv}{p} [1 - \exp(-pt_2)] \Omega, \quad t = t_2, \quad (5.30)$$

$$I_N = Bv \left[ \int_0^{t_2} \exp(-p(t-s)) ds - \int_{t_2}^{2t_2-t_1} \exp(-p(t-s)) ds \right] \Omega = \frac{Bv}{p} [2 \exp(pt_2) - \exp(p(2t_2 - t_1)) - 1] \exp(-pt) \Omega, \quad t \geq 2t_2 - t_1, \quad (5.31)$$

where  $t_1$  and  $t_2$  are the durations of portions  $OM_1$  and  $OM_2$ , respectively. The integral of non-homogeneity versus. time plot is shown in Figure 8(a). In particular, at  $t = 2t_2 - t_1$  ( $\sigma = \sigma_1$ , point  $N_2$  in Figure 6) Equation (5.31) gives

$$I_N = \frac{Bv}{p} [-1 - \exp(-p(2t_2 - t_1)) + 2 \exp(-p(t_2 - t_1))] \Omega. \quad (5.32)$$

Assuming that  $t_1 \rightarrow 0$  and  $t_2 \rightarrow 0$ , and following the reflections preceeding Equation (3.25), Equations (5.30) and (5.32) can be expressed as

$$I_N = BS_2 \Omega \text{ at point } M_2, \text{ and } I_N = BS_1 \Omega \text{ at point } N_2, \quad (5.33)$$

meaning that the integral of non-homogeneity changes in a step-wise way along  $OM_2N_2$ . Beyond point  $N_2$  (under the time independent stress  $\sigma_1$ ), we have (similarly to Equation (3.26a))

$$I_N = BS_1 \exp(-pt) \Omega. \quad (5.34)$$

According to Equation (5.14), the plastic strain intensity of Specimen No. 2 due to stress  $\sigma_2$  at point  $M_2$ , is

$$r\varphi_N = \psi_N = \bar{\mathbf{S}} \cdot \bar{\mathbf{N}} - I_N - S_P = S_2(1 - B)\Omega - S_P. \quad (5.35)$$

Since along  $M_2N_2$ , there is no plastic deformation, the defect/strain intensity remains unchangeable and is governed by (5.35). Consequently, Equations (A), (5.34), and (5.35) gives the plane distances at point  $N_2$ :

$$\begin{aligned} H_N &= \psi_N + I_N + S_P = S_2(1 - B)\Omega - S_P + BS_1\Omega + S_P \\ &= [S_2 - B(S_2 - S_1)]\Omega. \end{aligned} \quad (5.36)$$

Since  $0 \leq B < 1$ ,

$$H_N > \vec{\mathbf{S}} \cdot \vec{\mathbf{N}} = S_1\Omega, \quad (5.37)$$

meaning that the basic condition of the onset/development of irreversible straining-planes must be located on the end-point of stress deviator vector-is not satisfied. This means that the creep deformation does not start right after the stress has decreased from  $\sigma_1$  to  $\sigma_2$ , i.e., the phenomenon of *creep delay* is observed. The creep delay due to unloading is systematically observed in experiments performed by McLean [13], who stated that any fast enough decrease in acting stress always results in creep delay. The loading surface for Specimen No. 2 at point  $N_2$ , where the plane distances are given by Equation (5.36) is shown in Figure 7(c).

Inequality (5.37) expresses the hardening effect caused by the fact that Specimen No. 2 has incurred prior plastic deformation greater than for the case of conventional creep-loading,  $\varepsilon_2^S > \varepsilon_1^S$ .

If the irreversible strain does not progress, i.e.,  $d\varphi_N = 0$ , Equation (C) degenerates to the form of Equation (D) meaning that the defect relaxation starts:

$$\psi_N = [S_2(1 - B)\Omega - S_P] \exp(-Kt). \quad (5.38)$$

Inserting  $\psi_N$  from (5.38) and  $I_N$  from (5.34) into Equation (A), we obtain the following plane distances:

$$H_N = S_P + [S_2(1 - B)\Omega - S_P] \exp(-Kt) + BS_1 \exp(-pt)\Omega. \quad (5.39)$$

Hence, the planes move back in the direction of the creep surface, the

instant of time,  $t_d$ , when the first plane to be on the end-point of stress vector, is calculated by Equation (5.39) at  $\Omega = 1$  and  $H_N = S_1$ :

$$S_P + [S_2(1 - B) - S_P] \exp(-Kt_d) + BS_1 \exp(-pt_d) = S_1. \quad (5.40)$$

Time-period  $[0, t_d]$ , where  $t_d$  is determined from the above transcendental equation, is called the creep-delay. The loading surfaces at the beginning ( $t = t_d$ ) and development ( $t > t_d$ ) of creep deformation are shown in Figure 7(d) and 7(e), respectively.

As the vector  $\vec{S}$  reaches the plane with  $\Omega = 1$  at  $t = t_d$ , it starts producing irreversible (primary creep) deformation, and for this plane, the defects relaxation ceases. For other planes,  $\Omega < 1$ , the defects intensity continues to decrease according to Equation (5.38). Let us designate through  $t_z$  the instant of time, when the plane with  $\Omega < 1$  is on the end-point of  $\vec{S}$ . The time  $t_z$  is determined by Equation (5.39) at  $H_N = S_1\Omega$ :

$$S_P + [S_2(1 - B)\Omega - S_P] \exp(-Kt_z) + BS_1 \exp(-pt_z)\Omega = S_1\Omega. \quad (5.41)$$

Since Specimen No. 2 creeps under the same conditions as No. 1, Equations (5.18) and (5.21) remains valid. The only differences consists in that the strain intensity of Specimen No. 2 is positive as  $t > t_z$ , whereas for Specimen No. 1,  $\varphi_N \geq 0$  as  $t \geq 0$ , and  $t \geq t_0$  within the domain I and II, respectively. Therefore, the  $\varphi_N$  for Specimen No. 2 is determined by the time integration in Equation (5.21) in the limits from  $t_z$  to  $t$ :

$$\varphi_N = \int_{t_z}^t d\varphi_N. \quad (5.42)$$

$$\begin{aligned} r\varphi_N = S_1B \left(1 - \frac{K}{p}\right) (\exp(-pt_z) - \exp(-pt))\Omega \\ + K(S_1\Omega - S_P)(t - t_z), \quad t \geq t_z. \end{aligned} \quad (5.43)$$

Further, the strain vector component for Specimens No. 2 is calculated by the same integral as for Specimen No. 1 (the integral (5.22) within limits (5.19)), but now the integrand is given by Equation (5.43).

To compare the primary creep strain of Specimens No. 1 and No. 2, it is enough to analyze their strain intensities given by Equations (5.25) and (5.28) and Equation (5.43), respectively. The fact that the primary creep strain of Specimen No. 1 is greater than that of Specimen No. 2 can be substantiated by the following:

(1) At the beginning of creep, instants  $t = 0$  and  $t = t_z$ , respectively, there are the set of plane on the end-point of stress vector for Specimen No. 1 (Equation 5.23), and the sole plane for Specimen No. 2 (compare Figure 7(a) and 7(d)). This immediately means that, the development of primary creep for Specimen No. 1 starts more intensively than that for Specimen No. 2.

(2) The difference between Equations (5.25) and (5.28) and Equation (5.43) consists only in the value of times  $t_0$  and  $t_z$ . For Specimen No. 1,  $t_0 = 0$  for domain I, and the value of  $t_0$  is determined from Equation (5.26) for domain II. The value of  $t_z$  is determined by Equation (5.41). From the analysis of Equations (5.26) and (5.41), it may be inferred that  $t_z > t_0$ . This fact also implies that, the creep strain intensity of Specimen No. 2 is smaller than that of Specimen No. 1 in the course of primary creep. It must be noted that, if to set  $K = 0$ , Equations (5.26) and (5.41) become identical meaning that the simplified Equation (5.14) is incapable of modelling creep strains as a function of prior plasticity.

It is clear that the greater stress at prior plasticity. (points  $N_2$ ,  $N_3$ , and  $N_4$ ), the greater value of  $t_z$  meaning the progressive character of the decrease in primary creep strain. Therefore, the synthetic theory leads to the decrease in primary creep with the growth in prior plasticity.

Figure 9 shows experimental (Ohashi et al. [15]) and model creep diagrams, the latter are constructed on the base of Equations (5.25), (5.27), (5.28), and (5.29) for Specimen No. 1 and Equations (5.41), (5.43), and (5.22) for Specimen No. 2 with the following model constants:  $r = 4900\text{MPa}$ ,  $p = 0.5 \cdot 10^{-4} \text{ 1/sec}$ ,  $K = 7.55 \cdot 10^{-8} \text{ 1/sec}$ ,  $B = 0.235$ . The values of plastic pre-strains (see Table 1) are calculated by Equation (5.9), where the second term is set equal zero due to the assumption that the loading durations tend to zero.

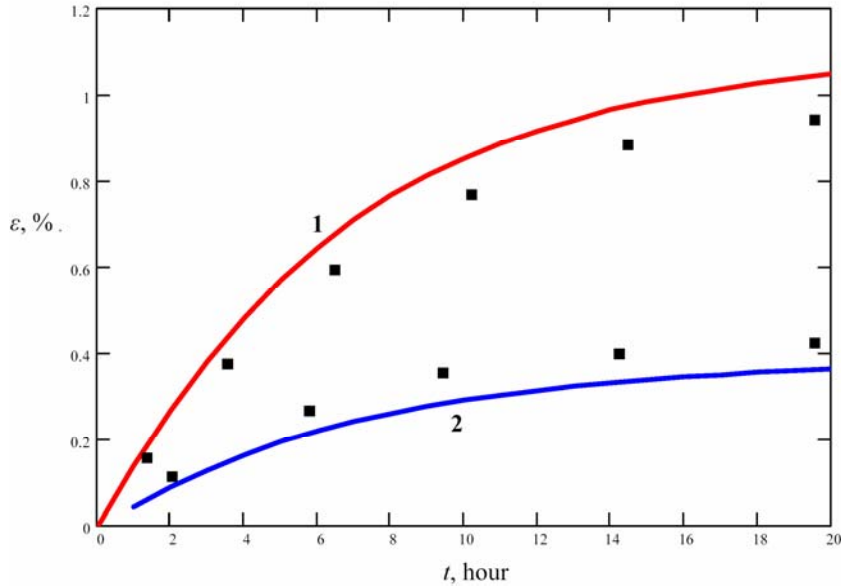


**Figure 9.** Creep diagrams of Specimens No. 1 and 2  $\sigma = 140\text{MPa}$ ,  $T = 650^\circ\text{C}$  (■ experimental points: Ohashi et al. [15]).

**Table 1.** Plastic pre-strains (points  $M_k (k = 1, \dots, 4)$  in Figure 6)

Stresses $\sigma_j$ at points $M_j (j = 1, \dots, 4)$ , MPa	Plastic strain, $\varepsilon_j^S (j = 1, \dots, 4)$ , %	
	Theory	Experiment
140	0.273	0.28
174	0.88	1.0
196	1.8	2.0
218	2.64	3.0

As one can see from Figure 9, the synthetic theory gives satisfactory agreement with experimental data.

## 6. Conclusion

The generalized synthetic theory of irreversible deformation is capable of modelling very wide circle of problems ranging from plastic

and steady/unsteady-state creep deformation to non-classical problems of irreversible deformation, such as the creep delay and the plastic-creep deformation interrelation. This capability results from (i) the uniformed approach to the modelling of irreversible deformation, and (ii) the effective connection between macro-deformation and the processes occurring on the macro-level of material.

### Acknowledgement

The author expresses thanks to Prof. K. Rusinko (Budapest University of Technology and Economics, Hungary) for many useful conversations on the topics presented in this article.

### References

- [1] J. Andrusik and K. Rusinko, Plastic strain of work-hardening materials under loading in three-dimensional subspace of five-dimensional stress-deviator space, (in Russian), *Izv. RAN (Russian Academy of Sciences), Mekh. Tverd. Tela* 2 (1993), 92-101.
- [2] R. J. Asaro and J. R. Rice, Strain localization in ductile single crystals, *Journal of the Mechanics and Physics of Solids* 25 (1977), 309-338.
- [3] R. J. Asaro, Micromechanics of crystals and polycrystals, *Advances in Applied Mechanics* 23 (1983), 1-115.
- [4] R. J. Asaro, Crystal plasticity, *Journal of Applied Mechanics* 501 (1983), 921-934.
- [5] J. Betten, *Creep Mechanics*, Springer, Berlin, 2005.
- [6] J. L. Chaboche, Unified Cyclic Viscoplastic Constitutive Equations: Development, Capabilities, and Thermodynamic Frame Work, *Unified Constitutive Laws of Plastic Deformation*, Krausz and Krausz eds, Academic Press, 1996.
- [7] J. L. Chaboche, P. M. Lesne and J. F. Maire, Thermodynamic formulation of constitutive equations and applications to the viscoplasticity and viscoelasticity of metals and polymers, *Int. J. Solid and Structures* 1997.
- [8] J. Chakrabarty, *Applied Plasticity*, Springer-Verlag, New York/Berlin/Heidelberg, 2000.
- [9] W. F. Chen and D. J. Han, *Plasticity for Structural Engineers*, New York, 1988.
- [10] J. Hutchinson, Plasticity at the micron scale, *Int. J. Solids and Structures* 37 (2000), 225-238.
- [11] A. A. Ilyushin, *Plasticity*, Moscow, 1963.

- [12] L. Kuksa, A. Lebedev and B. Koval'chuk, Laws of distribution of microscopic strains in two-phase polycrystalline alloys under simple and complex loading, *Strength of Materials* 18 (1986), 1-5.
- [13] D. McLean, *Mechanical Properties of Metals and Alloys*, John Wiley, New York and London, 1977.
- [14] S. Nemat-Nasser and T. Okinaka, A new computational approach to crystal plasticity: fcc single crystal, *Int. J. Mech. Mater.* 24 (1996), 43-57.
- [15] Y. Ohashi, M. Kawai and T. Momose, Effects of prior plasticity on subsequent creep of type 316 stainless steel at elevated temperature, *J. Eng. Mater. Technol.(Trans. ASME)* 108 (1986), 68-74.
- [16] D. Peirce, R. J. Asaro and A. Needleman, Material rate dependence and localized deformation in crystalline solids, *Acta Metallurgica* 31 (1983), 1951-1983.
- [17] Y. Rabotnov, *Creep Problems in Structural Members*, Amsterdam, North Holland/London, 1969.
- [18] A. Rusinko, Creep with temperature hardening, *J. Materials Science* 33 (1997), 813-817.
- [19] A. Rusinko, Bases and Advances of the Synthetic Theory of Irreversible Deformation, 22nd International Congress of Theoretical and Applied Mechanics (ICTAM) 25-29 August 2008, Adelaide, Australia, 2008.
- [20] A. Rusinko, Plastic-Creep Deformation Interrelation, 7-th EUROMECH Solid Mechanics Conference 7-11 September 2009, Lisbon, Portugal, 2009.
- [21] A. Rusinko and K. Rusinko, Synthetic theory of irreversible deformation in the context of fundamental bases of plasticity, *Int. J. Mech. Mater.* 41 (2009), 106-120.
- [22] E. Ruszinko, The influence of preliminary mechanical-thermal treatment on the plastic and creep deformation of turbine disks, *MECCANICA* 43 (2009), 13-24.

